Surface Science 213 (1989) 336–358
North-Holland, Amsterdam

ENERGY EXCHANGE IN ADSORBED LAYERS

O.M. BRAUN

Institute of Physics, Ukrainian Academy of Sciences, Kiev 252028, USSR

Received 11 May 1988; accepted for publication 1 September 1988

Various mechanisms of energy exchange between an adparticle (adatom, admolecule) and a substrate such as phonon, electron–hole and plasmon (electromagnetic) mechanisms are considered. It is shown that in some cases, for example for a light atom adsorbed on a semiconductor surface the rate of energy exchange is so small that the absolute rate theory is unsuitable. In these cases the nonlinear coupling between the degrees of freedom of the adsystem leads to stochastization of the motion of the adsystem. This stochastization causes (a) "dephasing" broadening of the vibrational line of the adsystem; (b) change of the temperature dependence of the rate of admolecule dissociation; and (c) the limitation on the free path motion of diffusing adparticles. It is pointed out that in the low friction case the role of the stimulated processes can be significant.

1. Introduction

Energy exchange between various degrees of freedom of an adsystem plays a significant role in all surface dynamical processes such as adsorption and desorption, inelastic scattering of particles, surface diffusion and crystal growth, heterogeneous catalytic reactions and so on. Usually, the rate of a dynamical process R is inversely proportional to the rate of energy exchange γ: $R \propto \gamma^{-1}$. However, as shown by Kramers [1], for an activated process (with an activation energy ϵ_b and a substrate temperature T such that $T \ll \epsilon_b$) and for a sufficiently small value of γ the opposite relationship holds: $R \propto \gamma$.

It is natural to begin the investigation of energy-exchange processes with the simplest case of vibrations of an adsorbed atom or molecule. It is convenient to classify that various mechanisms of vibrational damping according to the type of quasiparticles created in the substrate: phonons, electron–hole pairs, plasmons and so on. Thus phonon, electron–hole (e–h), and plasmon (electromagnetic) decay mechanisms are introduced. Certainly, this classification is rigorous as far as it is correct to treat the substrate as a noninteracting quasiparticles system. In section 2 we estimate the rate of energy exchange γ between the vibrations of the adparticle and other degrees of freedom with the help of the Green function technique. It will be shown that in some cases the rate γ is very small.

0039-6028/89/$03.50

For arbitrary motion of an adparticle it is convenient to describe the rate of energy exchange phenomenologically by a suitable friction coefficient. The methods of introducing the friction coefficient η are discussed in section 3.

In section 4 we consider three typical examples of surface dynamical processes such as adparticle vibrations near the minimum of the substrate potential, the escape rate of an adparticle from the potential well and diffusion of an adparticle in a periodic surface potential. The relationship between the friction coefficient η and the vibrational linewidth Γ, the escape rate R and the diffusion coefficient D is discussed.

In section 5 we give the conclusions and discuss the possibility of stimulated processes in the low friction case.

We shall use the atomic units system, $\hbar = m_e = e^2 = k_b = 1$, throughout.

2. Energy exchange for adparticle vibrations

Interest in the study of vibrations of atoms and molecules adsorbed on a crystal surface is caused by two reasons. Firstly, vibrational spectroscopy of adsorbates is a very informative method of investigation of adsystems (see surveys [2,3]). Secondly, the examination of local vibrations is the first step to the understanding of more complex surface dynamical processes.

Experimentally, the energy exchange between the substrate and adparticle vibrations can be measured directly or indirectly. The direct method uses picosecond laser pulses and measures the rate of decrease of the occupation number of the vibrational state (so-called "laser induced fluorescence" [4]). The usual spectroscopic methods described in ref. [5] are indirect as they measure the shape of the vibrational line $L(\omega)$ and the linewidth, Γ, which is connected with the rate of energy exchange γ. The function $L(\omega)$ is determined by the generalized susceptibility α of the adsystem [6]:

$$\begin{aligned} &L(\omega) \propto \operatorname{Im} \alpha(\omega), \\ &\alpha(\omega) = \int_{-\infty}^{+\infty} \mathrm{d}t \, \exp(\mathrm{i}\omega t) \alpha(t), \qquad (2.1) \\ &\alpha(t) = \mathrm{i}\theta(t) \langle \hat{P}(t)\hat{P}(0) - \hat{P}(0)\hat{P}(t) \rangle. \end{aligned}$$

Here $\hat{P}$ is the dynamical dipole moment operator, which is connected with the adparticle displacement $\hat{u}$ away from the equilibrium position: $P = e^* u$, where $e^* = \partial P / \partial u$ for $u = 0$. If the dynamical charge e^* is constant during vibrations, than $L(\omega) \propto \operatorname{Im} Q^{\mathrm{r}}(\omega)$, where Q^{r} is a usual retarded Green function for the adparticle displacements (the general case was considered by Langreth [7]).

2.1. Phonon decay of vibrational excitation

Let us consider the simplest case of an adatom vibrating perpendicular to the surface for A-type (atop-bonded) adsorption and take into account the interaction of the adatom with the neighbouring substrate atom only. If we denote the displacements of the adatom and the surface atom away from the equilibrium positions by u_a and u_s respectively, then the interaction energy H_{int} depends on their mutual displacement:

$$H_{int} = V(u), \quad u = u_a - u_s. \tag{2.2}$$

For the case of zero substrate temperature it is convenient to introduce a causal Green function

$$Q(t) = -i\langle \tilde{T} u(t) u(0) \rangle, \quad Q(\omega) = \int_{-\infty}^{+\infty} dt \exp(i\omega t) Q(t), \tag{2.3}$$

where $\tilde{T}$ is the time ordering operator.

The Green function (2.3) satisfies the Dyson equation

$$Q = Q_0 + Q_0 \Pi Q = (1 - Q_0 \Pi)^{-1} Q_0, \tag{2.4}$$

where the polarization operator $\Pi(\omega)$ is determined by the diagrams of fig. 1 and can be calculated by standard rules [6]. The advantage of using the Dyson equation consists in the possibility of taking into account various perturbations in the interaction H_{int} successively. For the zero-order approximation Q_0 we take the Green function of the system in the absence of interaction ($H_{int} = 0$):

$$Q_0(\omega) = m_a^{-1}(\omega^2 + i0)^{-1} + m_s^{-1} S(\omega). \tag{2.5}$$

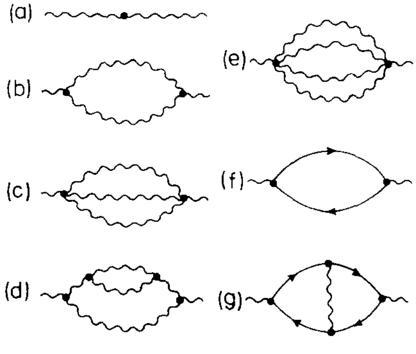

Fig. 1. Diagrams for the polarization operator $\Pi(\omega)$. Contributions are shown from the external potential (a), the decay into substrate phonons (b, c, d, e), and the decay into substrate e–h pair (f, g).

Here m_a and m_s are the masses of the adatom and the substrate atom respectively. The adsite Green function,

$$S(\omega) = -\mathrm{i}m_s\int_{-\infty}^{+\infty}\mathrm{d}t\,\exp(\mathrm{i}\omega t)\langle\tilde{T}u_s(t)u_s(0)\rangle, \tag{2.6}$$

is connected with the local density of phonon states near the surface, $\rho_b(\omega)$, by the relation

$$\rho_b(\omega) = -(2/\pi)\omega\,\mathrm{Im}\,S(\omega). \tag{2.7}$$

The simplest diagram shown in fig. 1a gives the contribution $\Pi_2 = V''(0) = \partial^2V(u)/\partial u^2\,|_{u=0}$ to the polarization operator and leads to the Green function in the harmonic approximation:

$$Q_h(\omega) = \frac{m_a^{-1}J(\omega)}{\omega^2 - \omega_a^2J(\omega) + \mathrm{i}0}, \quad J(\omega) = 1 + \frac{m_a}{m_s}\omega^2S(\omega), \tag{2.8}$$

where

$$\omega_a = (V''/m_a)^{1/2} \tag{2.9}$$

is the frequency of adatom vibrations on a "rigid" (immobile) substrate. Vibrations of substrate atoms cause a renormalization of the vibrational frequencies so that ω_0 is determined by solution of the equation

$$\omega_0^2 = \omega_a^2\mathrm{Re}\,J(\omega_0). \tag{2.10}$$

When the frequency ω_0 is lower than the maximum value ω_m of the vibrational frequency of the substrate atoms, the adatom vibrations are virtual and are characterized by the linewidth

$$\gamma = -\omega_0\omega_a^2(m_a/m_s)\,\mathrm{Im}\,S(\omega_0) = (\pi/2)(m_a/m_s)\omega_a^2\rho_b(\omega_0). \tag{2.11}$$

In the opposite case, $\omega_0 > \omega_m$, the vibrations are local and the contribution $\delta\Pi$ to the polarization operator, determined by the diagrams of figs. 1b–1g, leads to a shift of the vibrational frequency

$$\delta\omega = \left(\omega_0/2m_a\omega_a^2\right)\,\mathrm{Re}\,\delta\Pi(\omega_0) \ll \omega_0, \tag{2.12}$$

and to an increase of the vibrational linewidth

$$\gamma = \left(-\omega_0/m_a\omega_a^2\right)\,\mathrm{Im}\,\delta\Pi(\omega_0) \ll \omega_0. \tag{2.13}$$

Further on we shall use the Morse potential for $V(u)$:

$$V(u) = \epsilon_d[1 - \exp(-\kappa u)]^2, \tag{2.14}$$

where ϵ_d is the adsorption energy and $\kappa = \omega_a(m_a/2\epsilon_d)^{1/2}$. The rules of diagrammatic perturbation theory for calculating the rate γ in the case of local vibrations can be formulated in the following form [6,8]:

(1) a factor λ_n,

$$\lambda_n = -\mathrm{i}\,\partial^nV(u)/\partial u^n\,|_{u=0} \simeq \epsilon_d\omega_0^n(m_a/\epsilon_d)^{n/2}, \tag{2.15}$$

is associated with each vertex, in which n phonon lines meet; (2) the function $\mathrm{i}Q(\omega)$ corresponds to each phonon line (see wavy lines in fig. 1); for $\omega \lesssim \omega_\mathrm{m}$ in the case of $\omega_0 \gg \omega_\mathrm{m}$ it can be approximately modified according to

$$\begin{aligned} \mathrm{Im}\ Q_\mathrm{h} &\simeq -\left(\pi\omega^3\rho_\mathrm{h}(\omega)/2m_\mathrm{s}\omega_0^4\right) \\ &\simeq -\left(1/m_\mathrm{s}\omega_0^2\right)\left(\omega_\mathrm{m}/\omega_0\right)^2; \end{aligned} \tag{2.16}$$

(3) integration ($\int_{-\infty}^{+\infty} \mathrm{d}\omega'/2\pi$) is carried out with respect to the free energy parameters; this procedure approximately gives a factor of order ω_m.

For example, the simple phonon loop of fig. 1b, which describes the decay of the local vibration into two phonons, leads to the following contribution to the linewidth:

$$\gamma_2 \simeq r_0^2(\mathrm{Im}\ Q_\mathrm{h})^2\lambda_3^2\omega_\mathrm{m} \simeq \omega_0(m_\mathrm{a}/m_\mathrm{s})^2(\omega_0/\epsilon_\mathrm{d})(\omega_\mathrm{m}/\omega_0)^5, \tag{2.17}$$

where $r_0 = (2m_\mathrm{a}\omega_0)^{-1/2}$ is the amplitude of quantum vibrations. The decay of a local vibration into three phonons caused by a higher anharmonic term in H_int corresponds to an increase of the order of the vertex (see fig. 1c); as a result expression (2.17) is multiplied by a small parameter.

$$\xi \simeq (\mathrm{Im}\ Q_\mathrm{h})(\lambda_4/\lambda_3)^2\omega_\mathrm{m} \simeq (m_\mathrm{a}/m_\mathrm{s})(\omega_0/\epsilon_\mathrm{d})(\omega_\mathrm{m}/\omega_0)^3 \ll 1. \tag{2.18}$$

The decay of a local vibration into three phonons is also described by the next order of the perturbation theory (see fig. 1d); in this case expression (2.17) is multiplied by a small parameter

$$\xi' \simeq (\mathrm{Im}\ Q_\mathrm{h})^3\lambda_3^2\omega_\mathrm{m} \simeq (m_\mathrm{a}/m_\mathrm{s})^3(\omega_0/\epsilon_\mathrm{d})(\omega_\mathrm{m}/\omega_0)^7 \ll 1. \tag{2.19}$$

Comparing eqs. (2.18) and (2.19) we see that $\xi' \ll \xi$; therefore the higher orders of the perturbation theory can be neglected. For example, we can obtain for the H–W adsystem with $\omega_0^{(\perp)} \simeq 3.7\omega_\mathrm{m}$, $m_\mathrm{s}/m_\mathrm{a} = 184$, $\epsilon_\mathrm{d} \simeq 3$ eV and $\omega_\mathrm{m} \simeq 35$ meV the following estimate for the rate of the decay process of the adatom vibration into four substrate phonons (see fig. 1e): $\gamma \simeq \gamma_2\xi^2 \simeq 10^{-20}\omega_0$.

The decay probability of a local vibration into n phonons for $n \geqslant 2$ must essentially depend on the substrate temperature T because phonons are Bose-particles. With the help of the temperature-dependent Green function method [6] we obtain for the phonon loop of fig. 1b the expression:

$$\mathrm{Im}\ \Pi(\omega_0) = |\lambda_3|^2 Z(Q, Q; \omega_0), \tag{2.20}$$

$$\begin{aligned} &Z(Q_1, Q_2; \omega) \\ &\quad = \int_0^{\omega_m} (\mathrm{d}\omega'/\pi)\ \mathrm{Im}\ Q_1(\omega')\ \mathrm{Im}\ Q_2(\omega-\omega')\left[1+\nu(\omega')+\nu(\omega-\omega')\right] \\ &\qquad + \int_0^{\infty} (\mathrm{d}\omega'/\pi)\left[\mathrm{Im}\ Q_1(\omega')\ \mathrm{Im}\ Q_2(\omega+\omega')\right. \\ &\qquad \left. + \mathrm{Im}\ Q_1(\omega+\omega')\ \mathrm{Im}\ Q_2(\omega')\right]\left[\nu(\omega')-\nu(\omega+\omega')\right], \end{aligned} \tag{2.21}$$

where $\nu(\omega) = [\exp(\omega/T) - 1]^{-1}$ is the Bose distribution function. Neglecting the ω-dependence of $\mathrm{Im}\, Q(\omega)$ in the interval $\omega_0 - \omega_m < \omega < \omega_m$, one can obtain an approximate expression:

$$\gamma(T) = \gamma(0) A(T),$$

$$A(T) \simeq \frac{2T}{2\omega_m - \omega_0} \ln\left(\frac{\sinh(\omega_m/2T)}{\sinh[(\omega_0 - \omega_m)/2T]} \right), \tag{2.22}$$

thus at low temperatures $T \ll (\omega_0 - \omega_m)$

$$A(T) \simeq 1 + [2T/(2\omega_m - \omega_0)] \exp[-(\omega_0 - \omega_m)/T], \tag{2.23}$$

and at high temperatures $T \gg \omega_m$

$$A(T) \simeq [2T/(2\omega_m - \omega_0)] \ln[\omega_0/(\omega_0 - \omega_m)]. \tag{2.24}$$

Similarly, for the decay process into n phonons at high temperatures we have $\gamma(T) \propto T^{n-1}$.

Thus, the rate of the local vibration decay process into substrate phonons is, first of all, determined by the ratio ω_0/ω_m, and also by the anharmonicity of the interaction potential. The phonon decay mechanism plays an important role in the case $\omega_0/\omega_m \lesssim 2$–3.

2.2. Electron–hole decay

According to the well-known Gurney model [9] (see also ref. [10]) the electron wave functions of the adparticle and the metal hybridize when chemisorption takes place. As a consequence of this hybridization the initially discrete electron level ϵ_a of the adparticle is transformed into a virtual level of halfwidth Δ. When the adparticle vibrates perpendicular to the surface the position and the width of the virtual level are changed periodically. Because the position of the Fermi level ϵ_F is fixed, the vibrations cause a flow of electrons from the adparticle to the substrate and vice-versa. Due to the continuity of the substrate electron spectra the flow process proceeds non-adiabatically with the creation of electron–hole pairs in the substrate. If the adparticle, chemisorbed on a symmetric site at the surface, vibrates parallel to the surface, the electrons flow along the surface; this flow process leads also the creation of e–h pairs. It should be noted that the damping mechanism for perpendicular vibrations is often referred to as "charge transfer mechanism", whereas for parallel vibrations it is called "potential scattering mechanism" [11].

For the sake of simplicity we consider the case of chemisorption of an atom with a single non-degenerate electron orbital $|A\rangle$ which is mixed by the matrix elements $V_i = \langle A | H | i \rangle$ with the nearest substrate atom orbitals $|i\rangle$.

The Hamiltonian in the site-representation then takes the Anderson-type form [10]:

$$H = H_0 + H_{\text{int}}(u)$$
$$= H_s + (\epsilon_a + \epsilon' u) c_a^* c_a + \sum_i (V_i + V_i' u)(c_a^* c_i + \text{h.c.}). \tag{2.25}$$

Here H_s is the substrate electronic Hamiltonian, c and c^* are the Fermi operators and u is the relative shift in any direction. Now the rules of the diagrammatic perturbation technique are formulated as follows [6,8]: the function $\mathrm{i}G(\epsilon)$, $G(\epsilon) = (\epsilon - H_0 - \mathrm{i}0)^{-1}$, corresponds to the Fermionic line (in the diagrams of fig. 1 the Fermionic line is shown by a full line) and the factor $-\mathrm{i}\lambda$, $\lambda = \epsilon'$ or V_i', corresponds to each vertex.

Summing all the contributions from the diagram of fig. 1f with various indices (A, i) of Fermionic lines and summing over the electron spin, we obtain in the quasi-adiabatic approximation ($\Delta \gg \omega_0$) the following expression for the rate of e–h decay [12]:

$$\gamma = (2/\pi m_a)(B_\perp + B_\parallel), \tag{2.26}$$
$$B_\perp = \left\{ \pi\rho_a(\epsilon_F)\left[\epsilon' - (\epsilon_a - \epsilon_F)\Delta'/\Delta\right]\right\}^2,$$
$$B_\parallel = 2\pi\Delta\rho_a(\epsilon_F)\left\{\langle A|\bar{V}'\mathrm{Im}\,\bar{g}(\epsilon_F)\bar{V}'|A\rangle/\Delta - (\Delta'/2\Delta)^2\right\},$$

where $\rho_a(\epsilon) = \pi^{-1}\mathrm{Im}\langle A|G(\epsilon)|A\rangle$ is the local density of adatom electronic states. To simplify the notation we have used the matrix symbols:

$$\bar{V} = \{V_i\}, \quad \bar{V}' \equiv \{V_i'\}, \quad \bar{g} \equiv \{g_{ij}\},$$
$$g_{ij} = \langle i|g(\epsilon)|j\rangle, \quad g(\epsilon) = (\epsilon - H_s - \mathrm{i}0)^{-1}. \tag{2.27}$$

As an example we consider the case of B-type (bridge-bonded) adsorption (see fig. 2). Let us suppose that the adatom interacts with the nearest surface atoms 1 and 2 only, and that the dependence of the parameter V_i on the distance r between the adatom and the surface atom has the form

$$V_i(u) = V\exp\left[-(r - r_a)/\tilde{r}_a\right], \tag{2.28}$$

where $\tilde{r}_a \simeq r_a$, and $r_a = [d^2 + (a/2)^2]^{1/2}$ is the equilibrium distance (see fig. 2).

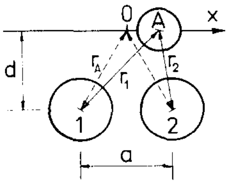

Fig. 2. B-type adsorption. A-adatom, 1 and 2-substrate atoms.

For the perpendicular adatom vibrations it follows from eq. (2.26) (for details see ref. [12]) that

$$\gamma_{\perp} \simeq \omega_0 4\pi(\delta n)^2 \simeq \omega_0 4\pi(e^* r_0/r_{\mathrm{d}})^2, \tag{2.29}$$

where $r_{\mathrm{d}} \simeq d$ is the distance from the adparticle to the surface and δn is the fluctuation in the occupation number of the valence electron orbital $|A\rangle$,

$$\delta n = r_0\left[\epsilon' - 2(\epsilon_{\mathrm{a}} - \epsilon_{\mathrm{F}})(V'/V)\right]\rho_{\mathrm{a}}(\epsilon_{\mathrm{F}}). \tag{2.30}$$

The value δn is connected with the experimentally measured dynamical dipole moment P_0 by the relation $P_0 = e^* r_0 \simeq (\delta n) r_{\mathrm{d}}$. For parallel adatom vibrations it follows that $\epsilon' = \Delta' = 0$ and $B_{\perp} = 0$ for reasons of symmetry. In this case we derive [12] from eqs. (2.26)–(2.28)

$$\begin{aligned}\gamma_{\parallel} &= 4\rho_{\mathrm{a}}(\epsilon_{\mathrm{F}})\tilde{\Delta}(V'/V)^2/m_{\mathrm{a}} \\ &\simeq (\omega_0/2)\tilde{\Delta}\rho_{\mathrm{a}}(\epsilon_{\mathrm{F}})\left[(r_0 a)/(r_{\mathrm{a}}\tilde{r}_{\mathrm{a}})\right]^2,\end{aligned} \tag{2.31}$$

where the value of $\tilde{\Delta}$ is determined by the electronic structure of the substrate:

$$\begin{aligned}&\tilde{\Delta} = \Delta\rho_{-}(\epsilon_{\mathrm{F}})/\rho_{+}(\epsilon_{\mathrm{F}}), \\ &\rho_{\pm}(\epsilon) = \pi^{-1}\,\mathrm{Im}\left[g_{11}(\epsilon) \pm g_{12}(\epsilon)\right].\end{aligned} \tag{2.32}$$

For chemisorption systems the following relations are usually satisfied: $e^* \lesssim 1$, $r_0 \approx 0.1$ a.u. and $r_{\mathrm{a}} \approx \tilde{r}_{\mathrm{a}} \approx a \approx d \approx r_{\mathrm{d}} \gtrsim 1$ a.u. It thus follows from eqs. (2.29) and (2.31) that for the e–h decay mechanism $\gamma_{\perp} \sim \gamma_{\parallel} \lesssim 10^{-2}\omega_0$. In the interesting case of hydrogen adsorption the dynamical adatom charge is usually small (for example, $e^* \simeq 0.053$ for H–W and $e^* \simeq 0.02$ for H–Si adsystems; see ref. [12] and references therein); therefore in this case the decay rate for perpendicular vibrations is extremely small: $\gamma_{\perp} \lesssim 10^{-3}\,\omega_0$.

Thus, electron–hole decay is the main mechanism for the case of chemisorption on metals if $\omega_0 \gg \omega_{\mathrm{m}}$. This mechanism is also efficient in the case of adsorption on semiconductor surfaces provided the density of surface electron states at the Fermi level, $\rho_{\mathrm{F}}(\epsilon_{\mathrm{F}})$, does not equal zero. The e–h mechanism has a simple isotopic effect: $\gamma \propto m_{\mathrm{a}}^{-1}$. During the e–h decay process a single boson (e–h pair) is predominantly created, so that the temperature dependence of $\gamma(T)$ is negligible [12].

2.3. Plasmon (electromagnetic) decay

When an adparticle dipole vibrates, an electromagnetic field is generated. This field penetrates into the substrate and creates quasiparticles such as surface plasmons, e–h pairs (so-called Landau damping) or optical phonons. The electromagnetic decay mechanism was discussed in a number of surveys (see refs. [2,3,13]). This mechanism can be efficient in cases when other damping mechanisms are ineffective, for example for physical adsorption of molecules with a high frequency of internal vibration ($\omega_0 \gg \omega_m$). The corresponding rate has a value $\gamma < 10^{-2}\omega_0$ (see ref. [2]).

It is obvious that electromagnetic damping is the main mechanism in the resonance case when the vibrational frequency ω_0 is close to an eigenfrequency of some substrate excitation ω_s. For example, for a semimetal or semiconductor with a static dielectric permeability ϵ_0, the frequency of the surface plasmons is equal to

$$\omega_s = \left[4\pi n/m^*(\epsilon_0 + 1)\right]^{1/2}, \tag{2.33}$$

where n is the concentration and m^* is the effective mass of the electrons or holes in the substrate. The value of n can be easily changed by heating the substrate or by laser pumping; thus the resonance case ($\omega_s = \omega_0$) can be achieved.

2.4. Interaction between local modes

In addition to energy transfer into the substrate, energy exchange between various vibrational modes of the adlayer is also possible. Let us now discuss these processes. Firstly, two identical atoms, adsorbed at points $\boldsymbol{r}_1$ and $\boldsymbol{r}_2$, always interact with some energy $U_{\mathrm{int}}(\boldsymbol{r}_1, \boldsymbol{r}_2)$. Different interaction mechanisms between adparticles such as direct, indirect, electrostatic (dipole–dipole) and elastic interactions were reviewed in ref. [14]. In the harmonic approximation these interactions lead to a shift in the vibrational frequency given by

$$\delta\omega \simeq r_0^2\left[\partial^2 U_{\mathrm{int}}/\partial u_1^2\right]_{u_1 = u_2 = 0}, \tag{2.34}$$

and to a frequency splitting

$$\omega_{\pm} = \omega_0 \pm \gamma, \quad \gamma \simeq r_0^2\left[\partial^2 U_{\mathrm{int}}/\partial u_1 \partial u_2\right]_{u_1 = u_2 = 0}. \tag{2.35}$$

If the first adatom is excited and the second is not, the value $\tau \simeq \gamma^{-1}$ defines the time of transfer of the excitation from the first adatom to the second. In the case of a regular adatom lattice γ determines the dispersion of the local vibrations. In the case of a random structure of the adatom layer the values $\delta\omega$ and γ determine the value of the inhomogeneous vibrational line broadening γ_x [3]. Estimates of γ for some adsystems were given in refs. [3,8] and lead to the value $\gamma \approx 10^{-2}\omega_0$.

It is necessary to point out that in general the interaction U_{int} includes a nonadiabatic contribution, which is caused by a delay in the response of the substrate to the moving adparticles. For example, for an electrostatic interaction the nonadiabatic contribution is large whenever the frequency ω_0 is close to the surface plasmon frequency ω_s. Moreover, the harmonic approximation used above is valid only for small displacements of the adatoms from their

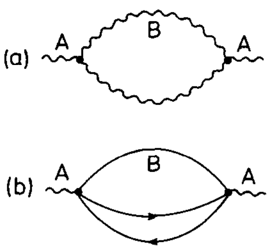

Fig. 3. Diagrams for the decay of local model A into another local mode B and the substrate phonon (a) or the e–h pair (b).

equilibrium positions. For large adatom vibrations the nonlinear interaction between adatoms and the finite value of the height of the surface potential should be taken into account. As a consequence, spatially localized modes such as the bion mode of the sine-Gordon equation always exist (see, for example, ref. [15]).

Finally, interaction between different modes exists even in the case of a single adatom, because the various vibrational modes of an adatom are always nonlinearly coupled due to the anharmonicity of the potential well. If this coupling is small the energy exchange between two modes can be described by the diagram of fig. 3a: the local model A decays into another local mode B and a substrate phonon. The substrate phonon takes away the difference of the mode energies, $\omega_{ab} = |\omega_a - \omega_b|$. For this process the rate of energy exchange, γ, is proportional to the local density of phonon states, $\rho_b(\omega_{ab})$, hence the condition $\omega_{ab} < \omega_m$ must be satisfied. Such processes were considered for S–Ni and O–Ni adsystems by Ariyasu et al. [16] and for H–W adsystem by Braun [17,18]. In ref. [17] the case when the excess of energy, ω_{ab}, is taken away by the substrate e–h pair (see diagram of fig. 3b) was also considered. Estimates [16–18] show that the rate γ has the value $\gamma \approx 10^{-2}\omega_0$.

The processes of figs. 3a and 3b correspond to the decay of the local vibration into two bosons; therefore the value of γ significantly depends on the substrate temperature T. If $\omega_a > \omega_b$, then it is easy to show from eqs. (2.20) and (2.21) that for the "down" decay process A → B

$$\gamma(T)/\gamma(0) \simeq 1 + \nu(\omega_b) + \nu(\omega_{ab}), \tag{2.36}$$

and for the "up" decay process B → A at $T \neq 0$

$$\gamma(T)/\gamma(0) \simeq \nu(\omega_{ab}) - \nu(\omega_a). \tag{2.37}$$

It is important to stress that for the case of energy exchange between local modes the vibrational excitation remains in the adlayer.

3. Friction coefficient

To describe the dynamics of an adsystem one often uses a trajectory approximation which treats the adparticle coordinate $x_a(t)$ as the coordinate of a classical particle. The force F,

$$F = \mathrm{d}p_a/\mathrm{d}t = -\mathrm{i}[p_a, H]_-,$$

$$p_a = m_a\dot{x}_a = -\mathrm{i}m_a[x_a, H] \ . \tag{3.1}$$

acts on the moving particle. The full force F can be divided into three parts:

$$F = F_a + F_r + F_f. \tag{3.2}$$

Both the adiabatic force F_a and the retarded force F_r are due to the creation of virtual quasiparticles with some frequency ω_s in the substrate. The value of F_a is calculated for the immobile adparticle located at the point $x = x_a(t)$. The last two parts of the force F depend on the whole previous trajectory of the adparticle. The contribution F_r is due to a delay in the response of the substrate to the moving particle. It is significant if $\omega_s \lesssim \omega_a$, where ω_a is some characteristic frequency of the motion of the adsystem (for example, ω_a can correspond to the frequency for which the correlation function, $K(\omega) = \int \mathrm{d}t\, \exp(\mathrm{i}\omega t)\langle\dot{x}(t)\dot{x}(0)\rangle$, reaches its maximum). For adparticle motion (excluding scattering processes) the contribution F_r can be usually ignored. The last term in eq. (3.2) is the friction force F_f, caused by the creation of real quasiparticles. For a small adparticle velocity v_a (for example, $v_a < \Delta k^{-1}_{\mathrm{Fermi}}$ for the e–h decay mechanism) the value of F_f is proportional to the velocity v_a.

Thus the motion of an adparticle can be described by the Langevin equation

$$m_a\ddot{x} - \langle F_a\rangle + m_a\int_0^{\infty} \mathrm{d}\tau\, \mu(\tau)\dot{x}(t-\tau) = \delta F(t), \tag{3.3}$$

where the fluctuation force $\delta F = F - \langle F\rangle$ satisfies the fluctuation-dissipation theorem [6]

$$\langle\delta F(T)\ \delta F(0)\rangle = m_a T\mu(t). \tag{3.4}$$

Following the well-known work of d'Agliano et al. [19] the parameters of eq. (3.3) must be chosen in such a way that in the simplest cases the adsystem characteristics, calculated from eq. (3.3) and the full quantum-mechanical theory, would coincide. For example, for harmonic oscillations of an adparticle with $\langle F_a\rangle = -m_a\omega_0^2 x$ we obtain from eq. (3.3) a Lorentz lineshape with the full width at half maximum

$$\Gamma = \mu(\omega_0) = \mathrm{Re}\int_0^{\infty} \mathrm{d}t\, \exp(\mathrm{i}\omega_0 t)\mu(t). \tag{3.5}$$

Therefore the value $\mu(\omega_0)$ should be identified with the value γ, which was calculated in section 2. However, it is important to note that the experimentally measured linewidth Γ always exceeds the rate of energy exchange γ (see ref. [3] and appendix A).

As was shown by Grote and Hynes [20] the non-Markovian Langevin equation (3.3) leads usually to the same results as the Markovian one with the suitably chosen value of the friction coefficient, $\eta \simeq \mu(\omega_a)$. A natural generalization of eq. (3.3), made in order to describe complex adparticle motion (such as diffusion), consists in using the coordinate-dependent friction coefficient $\eta(x)$:

$$m_a \ddot{x} + m_a \eta(x) \dot{x} - \langle F_a \rangle = \delta F(x, t), \tag{3.6}$$

$$\langle \delta F(x, t)\ \delta F(x, 0) \rangle = 2 m_a T \eta(x). \tag{3.7}$$

The parameter η introduced in such a way describes the rate of returning of the adsystem to the equilibrium state, whenever the displacement from the equilibrium state is small:

$$| E - \langle E \rangle | \simeq \langle E \rangle \exp(-\eta t), \tag{3.8}$$

where E is the energy of the adsystem. Correspondingly, the Langevin equation (3.6) describes dynamical processes near the equilibrium state such as vibrations or diffusion. However, for adsorption (sticking) or inelastic scattering processes the described technique can lead to a large error.

The regular procedure for calculating the effective friction tensor follows from eqs. (3.4) and (3.5):

$$\eta_{\alpha\beta}(x) = (m_a T)^{-1} \mathrm{Re} \int_0^\infty \mathrm{d}t\ \exp(\mathrm{i}\omega_a t) \langle \delta F_\alpha(x, t)\ \delta F_\beta(x, 0) \rangle_s. \tag{3.9}$$

Here $\langle \dots \rangle_s$ means that the average is taken over the substrate degrees of freedom for fixed position of the adparticle at the point x. The quantum generalization of expression (3.9) is given in appendix B.

The friction coefficient introduced above coincides with the rate of energy exchange, γ, which has been calculated in section 2. For example, for the e–h friction mechanism, from eq. (2.25) it follows

$$\delta F \simeq -\epsilon' c_a^* c_a - \sum_i V_i' (c_a^* c_i + \mathrm{h.c.}). \tag{3.10}$$

By substituting eq. (3.10) into eqs. (B.4)–(B.6) one obtains $\eta = \gamma$ where γ is determined by eq. (2.29) or (2.31) (see also ref. [21]). Following eq. (2.29), for perpendicular vibrations of the adparticle, the friction $\eta_\perp$ varies slowly as the adparticle moves along the surface. However , the parallel friction coefficient, $\eta_\parallel$, depends significantly on x. Taking the potential (2.28) and the geometry shown in fig. 2, eq. (2.31) yields the relationship

$$\frac{\eta_\parallel(x)}{\eta_\parallel(0)} \simeq \left[\frac{1}{2} \left(\frac{r_a}{r_1} + \frac{r_a}{r_2} \right) + \frac{x}{a} \left(\frac{r_a}{r_1} - \frac{r_a}{r_2} \right) \right]^2. \tag{3.11}$$

For the phonon friction mechanism the fluctuation force is

$$\delta F(u_a, u_s) = -\partial V(u_a, u_s)/\partial u_a, \tag{3.12}$$

where V is the energy of interaction between the adparticle and the substrate. As the simplest approximation we can assume

$$\delta F(u_s) \simeq V''(0) u_s, \tag{3.13}$$

where $V''(0) = m_a \omega_a^2$ according to eq. (2.9). From eqs. (B.4) and (2.6) it follows that $\eta = \gamma$, where γ is equal to the rate of one-phonon energy exchange (2.11). Of course, in this approximation $\eta = 0$ whenever $\omega_a > \omega_m$.

If the interaction potential, V, can be described by the Morse potential (2.14), the transition $|1\rangle \to |0\rangle$ of the adparticle in the potential well occurs due to the fluctuation force, $\delta F(u_s) = r_0 \langle 0 | V(u_a, u_s) | 1 \rangle$, and expression (B.4) for the friction coefficient can be evaluated exactly [22]. In this case all the important multiphonon processes are taken into account.

In the general case the correlation function, $\langle u_s(t) u_s(0) \rangle$, should be calculated self-consistently in such a way that the correlation between the motion of the adparticle and the substrate atoms is included (see ref. [23]). Similarly, in the quantum case expression (3.12) should be substituted into eq. (B.5); thus the friction coefficient, η, is expressed through the polarization operator, $\Pi(\omega_a)$. It is to be noted that the results of the self-consistent perturbation theory [8] differ from those of the non-self-consistent calculation [24,22] by the last factor in the expressions (2.16)–(2.19). As shown by Wahnström [23], the phonon friction coefficient, $\eta_{\parallel}(x)$, depends significantly on the position of the adparticle, x.

Following eq. (2.13), the full friction coefficient can be divided into two parts. One part is the "external" friction $\eta = \gamma$; it is described by the diagrams shown in figs. 1 and 3 and it is caused by energy exchange processes. The second part is the "internal" friction $\eta_t = \gamma_t$; it is represented by the "dephasing" diagrams (see appendix A) and it is closely related to the chaotization of the adparticle motion (see next section). The value of η_t is only significantly in the low friction case.

4. Rate of dynamical processes

Let us consider three typical examples of surface dynamical processes such as vibrations, dissociation and diffusion. They can be characterized by the following parameters: (a) the vibrations of an adatom or admolecule with frequency ω_0 can be described by the full width at half maximum Γ; (b) the dissociation of an adsorbed molecule can be characterized by the rate R; for activated processes the rate R usually takes the Arrhenius form

$$R = R_0 \exp(-\epsilon_b/T), \tag{4.1}$$

where ϵ_b is the activation energy; (c) the diffusion of an adparticle in the surface periodic potential $V(x)$ can be characterized by the diffusion coefficient D; it usually has the form

$$D = Rl^2, \tag{4.2}$$

where l is the mean free path of the adparticles.

In some cases it is convenient to use the Fokker–Planck–Kramers (FPK) equation for the distribution function $f(t, x, p)$ of coordinate x and momentum p of an adparticle:

$$\frac{\partial f}{\partial t} + \sum_{\alpha} \frac{p_\alpha}{m_a} \frac{\partial f}{\partial x_\alpha} - \sum_{\alpha} \frac{\partial V}{\partial x_\alpha} \frac{\partial f}{\partial p_\alpha} = \sum_{\alpha\beta} \frac{\partial}{\partial p_\alpha} \eta_{\alpha\beta}(x) \left(p_\beta f + m_a T \frac{\partial f}{\partial p_\beta} \right), \tag{4.3}$$

which is equivalent to the Langevin equation (3.6). Following Kramers [1], any dynamical process can be described by a one-dimensional FPK equation, if the coordinate x corresponds to the line which connects the saddle point and the minimum of the potential energy surface along the line of steepest descent. In our three cases the solutions of the one-dimensional FPK equation lead to the following results:

(a) Obviously, for a harmonic oscillator ($V(x) \propto x^2$), $\Gamma = \eta$. As shown by Renz and Marchesoni [25], in the case of an anharmonic oscillator, $\Gamma \gtrsim \eta$.

(b) The rate of dissociation, or the escape rate from the potential well was first calculated by Kramers [1]:

$$R_0 \simeq \begin{cases} \eta \epsilon_b / T & \text{for} \quad \eta \ll \eta_\ell = (\omega_0 / 2\pi)(T/\epsilon_b), \\ \omega_0 / 2\pi & \text{for} \quad \eta_\ell \ll \eta \lesssim \omega_0, \\ \omega_0^2 / 2\pi\eta & \text{for} \quad \eta \gtrsim \omega_0. \end{cases} \tag{4.4}$$

In the high friction case the reaction rate is limited by the diffusion of reagents in coordinate space. In the opposite case of low friction the reaction rate is limited by the diffusion in energy space (space of quantum numbers), because the distribution function is depleted (compared to the equilibrium function) by the particles with high energy. The result (4.4) was repeatedly verified in a number of works (see survey [26]). In the cases of adsorption of light atoms such as H, D or Li with $\eta \lesssim 10^{-2}\omega_0$ (see section 2) and $\epsilon_b \simeq 0.25$ eV (see ref. [27]) at room temperature, estimates give a value $\eta_\ell \simeq 10^{-2}\omega_0$; thus the regime of low friction can be acquired.

(c) The diffusion coefficient is determined by eqs. (4.2), (4.1) and (4.4), where in the intermediate and high friction cases we must put $l = a$ (a is a period of the surface potential). The low friction case when $l > a$ is more complicated. Following Risken and Vollmer [28] the "self-diffusion" coefficient in the equilibrium state is equal to

$$D_{\text{self}} = (\pi \epsilon_b / \eta m_a) \exp(-\epsilon_b / T). \tag{4.5}$$

This result is in accordance with eqs. (4.2) and (4.4), if $l = l_0 = \pi^{1/2} a\eta_f/\eta$. However, the "chemical-diffusion" coefficient, $D_{\text{chem}} = -j/q$, which relates the diffusion flux j and the gradient of adparticle concentration q, has opposite dependence on friction: $D_{\text{chem}} \propto \eta$ (see appendix C). In this case the adsystem is in a nonequilibrium state and the values j and q are only caused by deviation of the distribution function from its equilibrium form. Therefore the mean free path of the adparticles is reduced, $l < l_0$, due to the depletion of the distribution function by the high-energy particles [29].

It is obvious that for the adparticle motion we always have N degrees of freedom ($N \geqslant 3$), which are coupled due to the anharmonicity of the adsorption potential well. When the rate of energy exchange γ between the substrate and adlayer (adatom, admolecule) is large, $\gamma > \gamma_{\text{ex}}$, the energy exchange between adlayer modes proceeds through the substrate, and inclusion of other $(N-1)$ degrees of freedom leads only to a small correction to expression (4.4) for the reaction rate: $R \to RA$, where $A \simeq 1$ is the so-called entropy factor (see ref. [26]). However, in the case of low friction when the value of γ is lower than the rate γ_{ex} of energy exchange between adlayer modes (following section 2.4, $\gamma_{\text{ex}} \sim 10^{-2}\omega_0$) the nonlinear interaction between the modes becomes significant and leads to stochastization of the motion of the adparticle. We now discuss this case for our three typical processes separately.

4.1. Vibrations

The interaction between modes leads to dephasing broadening, γ_t, of the vibrational line. For example, the coupling of two modes (one perpendicular and one parallel to the surface) can be described by the Hamiltonian

$$H = \tfrac{1}{2} m_a \left(\dot{u}_\perp^2 + \dot{u}_\parallel^2 + \omega_\perp^2 u_\perp^2 + \omega_\parallel^2 u_\parallel^2 \right) + H_{\text{int}}, \tag{4.6}$$

where for symmetry reasons (see fig. 2)

$$H_{\text{int}} \propto u_\perp u_\parallel^2 . \tag{4.7}$$

The model (4.6), (4.7) belongs to the well-known Henon–Heiles type model [30]. On increasing the vibrational energy the adatom motion becomes stochastic and the nearest trajectories of motion in phase space become exponentially divergent with a rate which is equal to the so-called Kolmogorov–Sinai (KS) entropy h [30]. Therefore the time correlation function decays exponentially:

$$\langle u(t) u(0) \rangle \propto \exp(-\gamma_t t/2), \quad \text{with} \quad \gamma_t \propto h. \tag{4.8}$$

The dependence (4.8) in conjunction with eq. (2.1) leads to the linewidth broadening (A.1). A numerical estimate [18] for the H–W adsystem gives the value $\gamma_t \approx 10^{-2}\omega_0$. Calculation of γ_t by the diagrammatic perturbation technique is presented in appendix A.

4.2. Dissociation

As shown by Berne and co-workers [31], the escape rate in the low friction case is equal to

$$R_0 \simeq \frac{\eta(\epsilon_b/T)^N \Omega}{(N-1)!} \tag{4.9}$$

Here Ω is that part of phase space (from the whole available phase space) where the motion of the adsystem is chaotic.

4.3. Diffusion

The motion of the adparticle from one minimum of the potential energy to the next nearest one through the saddle point is the motion along the separatrix. Because of perturbations from other degrees of freedom the separatrix motion is always stochastic and has diffusion character even in the case $\eta \to 0$ [30]. Therefore as $\eta \to 0$, the mean free path, l, tends to some finite value l_m, which is determined by the KS-entropy h. In this case eqs. (4.2) and (4.9) yield the relationship

$$D_0 \propto \eta l_m^2/T^N. \tag{4.10}$$

It should be noted that for a curved trajectory of the adparticle the relationship $D \propto \eta$ was first predicted by Zhdanov [32].

5. Conclusion

In principle, the energy exchange mechanisms in the adlayer and in the bulk of a crystal are identical. The difference between the surface and bulk cases consists in fact that in the surface case the translation symmetry in the direction perpendicular to the surface is broken. This leads to the appearance of specific surface mechanisms such as high anharmonicity for phonon damping, charge-transfer processes for electron–hole damping, Landau creation of e–h pairs for electromagnetic damping mechanisms, and to the appearance of specific surface quasiparticles such as surface plasmons or electrons in surface states.

In the present work the rate of various decay mechanisms of vibrational excitation has been estimated. It was shown that in some cases the rate of energy exchange γ between the adlayer and the substrate is small. Namely, this situation takes place in the case of high adparticle vibration frequency (i.e., vibrations of a light adatom or the internal vibration of an admolecule) and small overlapping of electronic orbitals of the adparticle and substrate (i.e., the case of physical adsorption or chemisorption on a semiconductor surface with $\rho_F(\epsilon_F) \simeq 0$). In this regime the effect of stochastization plays a significant role and the rate of surface dynamical process R is proportional to the friction coefficient η. Of course, in these cases the rate R is sensitive to surface phase transitions and reconstructions.

In the case of slow energy exchange between the adlayer and substrate the adsystem is extremely sensitive to external effects. Irradiation of the surface by infrared light, by low energy electrons or by field emitted electrons will cause a transition of the adlayer to a nonequilibrium state. In this state stimulated surface processes such as desorption, diffusion, ordering and disordering can occur; and the rate of these processes can essentially exceed the equilibrium rate.

The energy of external excitation can be divided into two parts. One part is smoothed out between the adparticles (i.e., it is "chaotic" or "termalized"). This energy heats up the adlayer to some effective temperature $T_{\mathrm{eff}} > T$. Therefore the rate of surface dynamical processes is increased and becomes independent of the substrate temperature T. In ref. [33] it was supposed that the absence of temperature dependence of the diffusion coefficient at low temperatures $T \lesssim 130$ K for the H–W(110) adsystem, which was observed by DiFoggio and Gomer [34], can be explained in such a way. Similarly, the experimentally observed [35] ordering of the hydrogen layer adsorbed on the Mo(110) surface, when the adsystem is irradiated by a low energy electron beam, can be explained.

If the excitation happens locally in space, than the excitation energy remains localized during some short time $\tau \simeq \gamma^{-1}$. Moreover, a part of the excitation energy remains localized on the spatially local modes (such as bion mode, see ref. [15]) for a sufficiently long time. These excitations can lead to nonequilibrium transitions of adparticles from one adsite to the nearest unoccupied adsite; therefore defects can be created in an initially ordered adlayer. This process is similar to the well-known generation of defects in solids when they are exposed to external radiation.In this way the experimentally observed [35] electronically stimulated disordering process in H–Mo(110) and H–W(110) adsystems can be explained. Obviously, the rate of these stimulated processes should be proportional to the intensity of the irradiation beam, if saturation effects were absent.

Acknowledgements

I wish to thank Drs. A.G. Fedorus, A.G. Naumovets, E.A. Pashitskii, A.I. Volokitin and V.P. Zhdanov for useful discussions.

Appendix A: Dephasing broadening of the vibrational line

The experimentally measured linewidth Γ can be divided into three parts [3]:

$$\Gamma = \gamma + \gamma_x + \gamma_t. \tag{A.1}$$

Here γ is caused by energy exchange (see section 2). The inhomogeneous broadening, γ_x, is a result of the spatial chaos of the adsystem caused by defects (vacancies, steps, impurity atoms) of the crystal surface or adlayer. Finally, the effect of dephasing broadening, γ_t, is caused by the temporal chaos of the adsystem motion.

To calculate γ_t the diagrammatic perturbation technique is practicable. For example, the "self-action" diagram of fig. 4 describes the "elastic" scattering of quasiparticle X by the local vibrational mode A and leads to the following contribution to the polarization operator:

$$\operatorname{Im} \delta\Pi(\omega_0) = \lambda_4^2 b \int_0^{\omega_0^-} (\mathrm{d}\omega/\pi) \operatorname{Im} Q_X(\omega) \operatorname{Im} Q_X(\omega) A(\omega;\, T), \tag{A.2}$$

$$b \simeq \int_{\omega_0^-}^{\omega_0^+} (\mathrm{d}\omega/\pi) \operatorname{Im} Q_\mathrm{a}(\omega) \simeq r_{0\mathrm{a}}^2,$$

where

$$\omega_0^{\pm} \simeq \omega_0 \pm \Gamma$$

and

$$A(\omega;\, T) = \nu(\omega)[\nu(\omega) + 1].$$

If the quasiparticle X corresponds to a substrate phonon, then the rules of section 2 lead to the result (see also ref. [24]):

$$\gamma_t \simeq A(T)\,\omega_0 \left(\frac{m_\mathrm{a}}{m_\mathrm{s}}\right)^2 \left(\frac{\omega_0}{\epsilon_\mathrm{d}}\right)^2 \left(\frac{\omega_\mathrm{m}}{\omega_0}\right)^2, \tag{A.3}$$

where $A(T) \simeq (T/\omega_\mathrm{m})^2$. This estimate shows that "phonon" dephasing is not effective. However, the coupling of high-frequency mode A with the low-frequency mode B of the same adparticle is more effective. In this case $Q_X(\omega) \simeq r_{0\mathrm{b}}^2(\omega - \omega_\mathrm{b} - \mathrm{i}\Gamma_\mathrm{b})^{-1}$ near $\omega = \omega_\mathrm{b}$, and integration procedure (A.2)

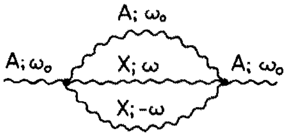

Fig. 4. Diagram for the dephasing process: elastic scattering of the local vibration A by a quasiparticle X.

leads to the factor Γ_b^{-1}. The corresponding contribution to the linewidth is given by the expression

$$\gamma_t \simeq 2A(\omega_b;\ T)(\lambda_4 r_{0a}^2 r_{0b}^2)^2/\Gamma_b$$
$$= 2A(\omega_b;\ T)(\delta\omega_{ab})^2/\Gamma_b, \qquad (A.4)$$

where $\delta\omega_{ab}$ is the shift in frequency of the A-mode when the B-mode is excited. Here $A(\omega_b;\ T) \simeq \exp(-\omega_b/T)$ at low temperatures, and $A(\omega_b; T) \simeq (T/\omega_b)^2$ at high temperatures. It should be pointed out that the density matrix method (see ref. [36]) leads to the same results.

If perturbation theory is used, chaos is introduced artificially when the averaging procedure is done. It is interesting to note that, contrary to the exact results (see ref. [18] and section 4), the third-order nonlinearity (4.7) in this case is not effective. Therefore, in order to obtain the correct value of γ_t an exact solution of the cluster motion equations must be made as has been done by Tully et al. [37]. The dephasing effect can be viewed as the process of changing the vibrational phase due to elastic scattering of the vibrations by another degree of freedom, or as the effect of fluctuations in the vibrational frequency [3]; both the events occur at random time.

Appendix B: Calculation of the friction coefficient

Of course, in quantum theory the friction coefficient can only be introduced phenomenologically. One way used by Volokitin [38] consists in calculating the full force (3.1) and extracting the term proportional to the velocity of the adparticle. We will use another method of d'Agliano et al. [19] based on linear response theory. Let us suppose that an adparticle moves along the trajectory $x(t)$ and is subjected to a fluctuation force δF. This action can be described by the operator

$$\hat{H}_{\text{int}} = -x(t)\delta\hat{F}. \qquad (B.1)$$

We introduce the generalized susceptibility according to the definition

$$\langle\delta F(t)\rangle = \int_0^\infty \mathrm{d}\tau\, \beta(\tau) x(t-\tau). \qquad (B.2)$$

The imaginary part of the Fourier transformation of the function $\beta(t)$ is equal to (see ref. [6])

$$\operatorname{Im}\beta(\omega) = \tfrac{1}{2}\tanh(\omega/2T)\int_{-\infty}^{+\infty} \mathrm{d}t\, \exp(\mathrm{i}\omega t)\langle\delta\hat{F}(0)\delta\hat{F}(t) + \text{h.c.}\rangle_s. \qquad (B.3)$$

If the adparticle vibrates near the point x with some amplitude x_a and frequency ω_a, $x(t) = x + x_a \sin(\omega_a t)$, then it loses its energy with the rate $\langle\dot{E}\rangle = \frac{1}{2}\omega_a x_a^2 \operatorname{Im}\beta(\omega_a)$. The total energy of the harmonic vibrations is equal to $\langle E \rangle = \frac{1}{2} m_a \omega_a^2 x_a^2$. Following eq. (3.8) we now introduce the friction coefficient with the help of the relation $\eta = \langle \dot{E} \rangle / \langle E \rangle$. Thus, the desired expression is:

$$\eta(x) = \frac{1}{2 m_a \omega_a} \tanh\left(\frac{\omega_a}{2T} \right) \int_{-\infty}^{+\infty} \mathrm{d}t \, \exp(\mathrm{i} \omega_a t) \langle \delta \hat{F}(0) \delta \hat{F}(t) + \mathrm{h.c.} \rangle_s . \tag{B.4}$$

In the classical case ($T \gg \omega_a$) eq. (B.4) reduces to eq. (3.9).

In the trajectory approximation the symbol

$$\langle \ldots \rangle_s = \mathrm{Sp}[\exp(-H_s/T) \ldots] / \mathrm{Sp}[\exp(-H_s/T)]$$

means the average over the independent motion of the substrate atoms. Generalization of the trajectory approximation uses the fact that the motion of the substrate atoms is correlated with the adparticle motion:

$$\langle \ldots \rangle_s \to \langle \ldots \rangle_{(\mathrm{full})} = \mathrm{Sp}[\exp(-H/T) \ldots] / \mathrm{Sp}[\exp(-H/T)] .$$

Then the friction coefficient, η, can be related to the causal Green function:

$$\eta = -(m_a \omega_a)^{-1} \tanh(\omega_a / 2T) \, \mathrm{Im} \, \tilde{Q}(\omega_a; T), \tag{B.5}$$

$$\tilde{Q}(t; T) = -\mathrm{i} \langle \tilde{T} \delta \hat{F}(t) \delta \hat{F}(0) \rangle .$$

Of course, in this case η depends on the whole previous trajectory of the adparticle and therefore must be calculated self-consistently. We recall (see ref. [6]) that for a system of noninteracting Bose-particles (phonons or e–h pairs)

$$\tanh(\omega / 2T) \, \mathrm{Im} \, \tilde{Q}(\omega; T) = \mathrm{Im} \, \tilde{Q}(\omega; 0). \tag{B.6}$$

Appendix C: "Chemical" diffusion in a one-dimensional periodic potential

In order to solve the one-dimensional FPK equation (4.3) we will use the fact that this equation has on exact stationary (but nonequilibrium) solution for the harmonic potential $U(x) = \pm \frac{1}{2} m \omega^2 x^2$ (see ref. [1]):

$$f_{\pm}(x, p) = \exp\left[-(p^2 / 2mT) - U(x)/T \right] \left[C_1 - C_2 \, \mathrm{Re} \, \varphi_{\pm}(x, p) \right], \tag{C.1}$$

where C_1 and C_2 are arbitrary constants,

$$\varphi_{\pm}(x, p) = \phi_{\pm}(p \alpha_{\pm} - x s \alpha_{\pm}^{-1}),$$

$$s = \omega^2 / 2 \eta T,$$

$$\alpha_{\pm}^2(\omega) = \pm (4mT)^{-1} \left[1 - (1 \mp 4 \omega^2 / \eta^2)^{1/2} \right],$$

and

$$\phi_{\pm}(z) = (2/\sqrt{\pi}) \int_0^z \mathrm{d}t \, \exp(\pm t^2)$$

are error functions. The distribution function (C.1) leads to the density of particles

$$\rho_\pm(x) = \int_{-\infty}^{+\infty} \mathrm{d}p f_\pm(x, p)$$

$$= (2\pi m T)^{1/2} \exp[-U(x)/T]\left[C_1 - C_2\phi_\pm\left(x\omega\sqrt{m/2T}\right)\right], \tag{C.2}$$

and to the constant flux of particles

$$j_\pm = m^{-1} \int_{-\infty}^{+\infty} \mathrm{d}p p f_\pm(x, p)$$

$$= C_2\left(4mT^2\eta/\omega\right) \operatorname{Re} \alpha_\pm^2. \tag{C.3}$$

At $\eta < 2\omega$, α_+ and the function $\varphi_+(x, p)$ become complex. In this case due to linearity of the FPK equation we will take the real part of the solution only.

Now let us construct the periodic potential $V(x)$ by periodic repetition of the following function, determined in the interval $(-x_0, a - x_0)$:

$$V(x) = \begin{cases} \epsilon_b - m\omega_b^2 x^2/2 & \text{for} \quad |x| \leqslant x_c, \\ (m\omega_a^2/2)(x - a/2)^2 & \text{for} \quad x_c < x < a - x_c, \end{cases} \tag{C.4}$$

where

$$x_c = a\frac{\omega_a^2 - \left[\omega_c^2\left(\omega_a^2 + \omega_b^2\right)/2 - \omega_a^2\omega_b^2\right]^{1/2}}{2\left(\omega_a^2 + \omega_b^2\right)},$$

$$\omega_c = (4/a)(\epsilon_b/m)^{1/2}.$$

The resulting periodic potential has period a and height ϵ_b (see fig. 5). In the intervals, where the potential $V(x)$ is harmonic, the solution of the FPK equation has the form (C.1) with the corresponding values of $\omega = \omega_a$ or ω_b.

Joining the solutions (C.1) at the points $x = \pm x_c + na$, $n = 0, \pm 1, \ldots$ in such a way that the density (C.2) and flux (C.3) of particles are continuous, we obtain the exact stationary solution of the FPK equation. It is characterized by

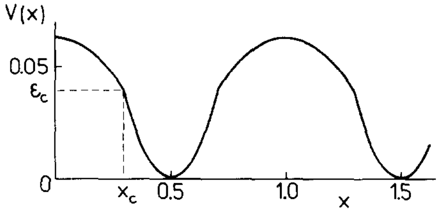

Fig. 5. Surface potential (C.4).

the constant flux j and the mean gradient of the concentration of particles, which is determined by

$$q=(1/a)\left(\int_0^a-\int_{-a}^0\right)(\mathrm{d}x/a)\ \rho(x). \tag{C.5}$$

By introducing the diffusion coefficient according to the relation $j=-Dq$, the following relationship of the diffusion and friction coefficients is obtained:

$$D=\left(a^2\omega_\mathrm{a}/2\pi\right)B(\eta)\ \exp(-\epsilon_\mathrm{b}/T), \tag{C.6}$$

where

$$B(\eta)=\eta\omega_\mathrm{b}K_+K_-/2L_1L_2,$$

$$K_+=4mT\ \mathrm{Re}\ \alpha_+^2(\omega_\mathrm{a}),$$

$$K_-=4mT\alpha_-^2(\omega_\mathrm{b});$$

$$L_1=\omega_\mathrm{a}\ \exp(-\epsilon_\mathrm{b}/T)\phi_+(y_2)K_-+\omega_\mathrm{b}\phi_-(y_1)K_+,$$

$$L_2=\omega_\mathrm{a}\ \exp(-\epsilon_\mathrm{b}/T)\phi_+(y_1)+\omega_\mathrm{b}\phi_-(y_2),$$

$$y_1=\sqrt{(\epsilon_\mathrm{b}-\epsilon_\mathrm{c})/T},\quad y_2=\sqrt{\epsilon_\mathrm{c}/T},$$

$$\epsilon_\mathrm{c}=\left(m\omega_\mathrm{a}^2/2\right)\left(a/2-x_\mathrm{c}\right)^2.$$

At low temperatures, $T \ll (\epsilon_\mathrm{c},\ \epsilon_\mathrm{b}-\epsilon_\mathrm{c})$, from eq. (C.6) it follows:

$$B(\eta)\simeq\begin{cases}\eta/\eta_\mathrm{c} & \text{for}\quad \eta\ll\eta_\mathrm{c},\\ 1 & \text{for}\quad \eta_\mathrm{c}\ll\eta\ll\omega_\mathrm{b};\\ \omega_\mathrm{b}/\eta & \text{for}\quad \eta\gg\omega_\mathrm{b},\end{cases} \tag{C.7}$$

where

$$\eta_\mathrm{c}\simeq 2\omega_\mathrm{b}(T/\pi\epsilon_\mathrm{c})^{1/2}\exp\left[-(\epsilon_\mathrm{b}-\epsilon_\mathrm{c})/T\right]. \tag{C.8}$$

At high temperatures, $T \gg \epsilon_\mathrm{b}$, eq. (C.6) leads to

$$D\simeq\begin{cases}\left(\eta T/2m\omega_\mathrm{a}^2\right)\left[a/(a-2x_\mathrm{c})\right] & \text{for}\quad \eta\ll\omega_\mathrm{a},\ \omega_\mathrm{b},\\ T/m\eta & \text{for}\quad \eta\gg\omega_\mathrm{a},\ \omega_\mathrm{b}.\end{cases} \tag{C.9}$$

References

[1] H.A. Kramers, Physica 7 (1940) 284.
[2] P. Avouris and B.N.J. Persson, J. Phys. Chem. 88 (1984) 837.
[3] J.W. Gadzuk and A.C. Luntz, Surface Sci. 144 (1984) 429.
[4] A. Laubereau, D. von der Linde and W. Kaiser, Phys. Rev. Letters 28 (1972) 1162.
[5] R.F. Willis, Ed., Vibrational Spectroscopy of Adsorbates (Springer, Berlin, 1980).

[6] L.D. Landau and E.M. Lifshitz, Statistical Physics, Part 1 (Nauka, Moscow, 1976); Part 2 (Nauka, Moscow, 1978);
L.P. Kadanoff and G. Baym, Quantum Statistical Mechanics (Plenum, New York, 1962).
[7] D.C. Langreth, Phys. Rev. Letters 54 (1985) 126.
[8] O.M. Braun and E.A. Pashitskii, Fiz. Tverd. Tela 24 (1982) 1973 [Soviet Phys.-Solid State 24 (1982) 1127]; Poverkhnost 6 (1984) 5 [Phys. Chem. Mech. Surfaces 3 (1985) 1587].
[9] R.W. Gurney, Phys. Rev. 47 (1935) 479.
[10] P.W. Anderson, Phys. Rev. 124 (1961) 41;
D.M. Newns, Phys. Rev. 178 (1969) 1123.
[11] B. Hellsing, Surface Sci. 152/153 (1985) 826.
[12] O.M. Braun and A.I. Volokitin, Fiz. Tverd. Tela 28 (1986) 1008 [Soviet Phys.-Solid State 28 (1986) 564].
[13] B. Gumhalter, Progr. Surface Sci. 15 (1984) 1.
[14] T.L. Einstein, CRC Crit. Rev. Solid State Mater. Sci. 7 (1978) 261.
[15] K. Lonngren and A. Scott, Eds., Solitons in Action (Academic Press, New York, 1978).
[16] J.C. Ariyasu, D.L. Mills, K.G. Lloyd and J.C. Hemminger, Phys. Rev. B 28 (1983) 6123; B 30 (1984) 507.
[17] O.M. Braun, Poverkhnost 11 (1987) 5.
[18] O.M. Braun, Radiophysics 30 (1987) 788 [Soviet Phys.-Radiophys. Quantum Electron. 30 (1987) 590].
[19] E.G. d'Agliano, P. Kumar, W. Schaich and H. Suhl, Phys. Rev. B 11 (1975) 2122.
[20] R.F. Grote and J.T. Hynes, J. Chem. Phys. 73 (1980) 2715.
[21] A. Nourtier, J. Phys. (Paris) 38 (1977) 479;
A. Yoshimori and J.-L. Motchane, J. Phys. Soc. Japan 51 (1982) 1826.
[22] A.I. Volokitin, O.M. Braun and V.M. Yakovlev, Suface Sci. 172 (1986) 31.
[23] G. Wahnström, Surface Sci. 159 (1985) 311.
[24] B.N.J. Persson, J. Phys. C (Solid State Phys.) 17 (1984) 4741.
[25] W. Renz and F. Marchesoni, Phys. Letters A 112 (1985) 124.
[26] P. Hänggi, J. Statist. Phys. 42 (1986) 105.
[27] A.G. Naumovets and Yu.S. Vedula, Surface Sci. Rept. 4 (1984) 365.
[28] H. Risken and H.D. Vollmer, Z. Phys. B 35 (1979) 177.
[29] V.I. Mel'nikov and S.V. Meshkov, J. Chem. Phys. 85 (1986) 1018.
[30] A.J. Lichtenberg and M.A. Lieberman, Regular and Stochastic Motion (Springer, Berlin, 1983).
[31] M. Borkovec and B.J. Berne, J. Chem. Phys. 82 (1985) 794;
J.E. Straub and B.J. Berne, J. Chem. Phys. 85 (1986) 2999.
[32] V.P. Zhdanov, Poverkhnost 4 (1986) 32.
[33] O.M. Braun and E.A. Pashitskii, Poverkhnost 7 (1984) 49 [Phys. Chem. Mech. Surface 3 (1985) 1989].
[34] R. DiFoggio and R. Gomer, Phys. Rev. B 25 (1982) 3490.
[35] V.V. Gonchar, Yu.M. Kagan, O.V. Canash, A.G. Naumovets and A.G. Fedorus, JETF 84 (1983) 249 [Soviet Phys.-JETP 57 (1983) 142];
V.V. Gonchar, O.V. Canash and A.G. Fedorus, Pisma JETF 38 (1983) 162 [JETP Letters 38 (1983) 189].
[36] R.M. Shelby, C.B. Harris and P.A. Cornelius, J. Chem. Phys. 70 (1979) 34.
[37] J.G. Tully, Y.J. Chabal, K. Raghavachari, J.M. Bowman and R.R. Lucchese, Phys. Rev. B 31 (1985) 1184.
[38] A.I. Volokitin, Poverkhnost 6 (1987) 30.